



Solvothermal growth of 3D flower-like CoS@FTO as high-performance counter electrode for dye-sensitized solar cell

Sajid Ali Ansari^{1,2} · Hemraj Yadav¹ · Muhammad Adeel¹ · Kicheon Yoo¹ · Jae-Joon Lee¹

Received: 24 November 2018 / Accepted: 22 February 2019 / Published online: 2 March 2019
© Springer Science+Business Media, LLC, part of Springer Nature 2019

Abstract

In this work, a simple and one-step solvothermal method has been developed for directly growing three-dimensional flower-like cobalt sulfide (CoS) on the fluorine-doped tin oxide coated glass substrate (FTO) for the counter electrode in the dye sensitized solar cell. The electrocatalytic activity of the CoS@FTO towards the I_3^- to I^- reduction exhibited almost similar electrocatalytic properties to the Pt-based counter electrode. The dye-sensitized solar cell (DSSC) assembled with CoS@FTO counter electrode attained almost similar photovoltaic performance (5.64%) to that of the DSSC with Pt@FTO counter electrode (5.9%) under 1 sun illumination. The adhesion stability of the CoS deposited at FTO was also studied using strong adhesive tape test, and the results show that after the strong adhesive tape test, the CoS@FTO retained almost 95% of the coating. The similar and comparative performance of the CoS@FTO to the Pt@FTO may be due to the high surface area originating from the 3D flower-like morphology, and the excellent electrocatalytic activity of the CoS.

1 Introduction

The extensive use of fossil fuel energy resources for various purposes has resulted in special attention in recent years being given to developing or building alternatives for future energy consumption [1–3]. For this purpose, researchers have focused on the utilization of solar cell energy using various types of photovoltaic device that can convert solar energy into electrical energy. Among them, the dye-sensitized solar cell (DSSC) has attracted much attention, due to its low cost, easy fabrication of oxides, and easy tunable characteristics [1–15].

The dye-sensitized titanium dioxide (TiO_2) photo anode, platinum (Pt) counter electrode, and I^-/I_3^- redox couple are the basic components of the DSSC. Among these, the

counter electrode i.e. Pt, has played an important role in collecting the electrons and catalyzing the redox reaction of the electrolyte. Another advantage of Pt is its excellent conductivity, various catalytic sites, and easy synthesis over the conducting substrate [1–3, 9]. However, despite the large number of advantages of the Pt counter electrode, the corroding behavior during the redox reaction, high cost, and lesser natural abundance are major drawbacks for its effective utilization as a counter electrode in the DSSC [1–3, 9, 10, 16, 17]. In this respect, various efforts have been devoted to developing an alternative to Pt as the counter electrode in DSSC, such as metal sulfide, metal selenide, and metal nitride. Among various metal sulfides, cobalt sulfide (CoS) has received special attention in DSSC, due to its high catalytic activity towards the redox reaction of the electrolytes, and simple synthesis process [1–3, 9, 10, 16–20].

For this purpose, various methods have been used to prepare CoS, which have their own advantages and disadvantages in terms of the various steps involved in the synthesis process: use of excess chemical, whose discharge may directly or indirectly affect the environment; and complicated synthetic steps.

For example Tsai et al. [3] demonstrated the fabrication of cobalt sulfide nanotube arrays on FTO-coated by combining three simple technologies (the selective etching of ZnO sacrificial templates, mesoporous Co_3O_4 formation from cobalt-chelated chitosan, and ion-exchange reaction);

Electronic supplementary material The online version of this article (<https://doi.org/10.1007/s10854-019-01008-6>) contains supplementary material, which is available to authorized users.

✉ Jae-Joon Lee
jjlee@dongguk.edu

¹ Department of Energy & Materials Engineering, Research Center for Photoenergy, Harvesting & Conversion Technology (phct), Dongguk University, Seoul 04620, Republic of Korea

² Present Address: Department of Physics, College of Science, King Faisal University, Al-Ahsa 31982, Saudi Arabia

whereas Tsai et al. [18] reported the ion exchange reaction of $\text{Co}(\text{OH})_2$ to prepare cobalt sulfide, and further tested its catalytic performance in the DSSC. Similarly, Congiu et al. [19] reported the synthesis of CoS using cobalt (II) bis-diethyl dithiocarbamate in chloroform. Thus, the need for a scalable, facile, and easy method that can be used for large-scale production is needed. Compared to the above mentioned method, a simple and one-step synthesis process directly growing CoS@FTO is considered to be a good and efficient method, compared to the other methods. Another advantage of directly growing CoS@FTO, instead of the suspension of the materials, is that it is helpful to avoid aggregation, detachment from the collector, and precipitation that directly influence the performance and stability of the device [1–3, 9, 10, 16–20]. Therefore in this work, a simple and one-step solvothermal method was employed to grow a three-dimensional flower-like cobalt sulfide on fluorine-doped coated glass (CoS@FTO), using aniline monomer as adhesive and directing agent. The developed CoS@FTO was characterized by spectroscopic and diffraction techniques, and its electrochemical and counter electrode performance in DSSC were further examined. The initial electrocatalytic activity towards the redox reaction of I^-/I_3^- measured by CV and the power conversion efficiency of the CoS@FTO are nearly the same as those of the well-studied and bench mark catalyst of Pt@FTO.

2 Experimental

2.1 Materials

Cobalt nitrate, aniline monomer, and Mucosal detergent were acquired from Sigma Aldrich. Thiourea was purchased from Alfa Acer. Fluorine-doped tin oxide (FTO, Pilkington TEC Glass-TEC 8, Solar, 2.3 mm thickness) glass was used as the substrate. TiO_2 paste was purchased from Dyesol Industries Pvt. Ltd., Australia. The dye N719 (cis-bis(isothiocyanato)-bis(2,20-bipyridyl-4,40-dicarboxylato)-ruthenium(II)bis-trabutylammonium), 1-propyl-3-methylimidazolium iodide (PMII), iodine (I_2), 4-tert-butylpyridine (tBP), acetonitrile, and lithium iodide were acquired from Sigma-Aldrich.

2.2 Methods

The crystal structure and phase characterization measurement was carried out using PANalytical X-ray diffractometry (X'pert PRO-MPD, Netherland) with $\text{Cu K}\alpha$ radiation ($\lambda = 0.15405$ nm), using a conventional electrochemical workstation with three electrode setup (CHI-430A, CH Instruments, USA). Platinum, Ag/AgCl, and CoS@FTO were used as counter, reference, and counter electrode, respectively. The thickness of the photoelectrode was measured by SURFCOM130A

surface profiler (Accretech Korea Co. Ltd). The solar simulator (Polaronix K201, Mc Science, Korea) was equipped with 200 W Xenon lamp, and the intensity of the illumination was $100 \text{ mW}/\text{cm}^2$. The power of the solar simulator was calibrated with the mono-Si standard solar cell (PVM-396), which is certified by the National Energy Laboratory, USA. The IV characteristic was measured by KETHLEY interlinked with the Oriel Instrument software. The electrolyte was prepared by dissolving 0.6 M of PMII, 0.1 M LiI, 0.03 M I_2 , and 0.5 M tBP in acetonitrile solvent.

2.3 Synthesis of CoS@FTO

Before the synthesis of CoS@FTO, FTO was cleaned in ultrasonic bath using detergent, water, and ethanol. For the synthesis of CoS@FTO, 250 μL of the aniline monomer was mixed using ultrasonication in 40 mL ethanol. After that, 1 g of the cobalt nitrate was dissolved in the above solution, and sonicated for 5 min. Then 0.5 g of the thiourea was added as sulfur source in the above mixture, and the mixture was further sonicated for 5 min. Subsequently, the above mixture was transferred into the Teflon-lined autoclave, and the cleaned FTO glass was placed at an angle against the wall of the Teflon, with the FTO-coated face down. The whole system above was sealed, and heated at 200 °C for 12 h. After the reaction was completed, the autoclave was cooled to room temperature, and the coated CoS@FTO was rinsed with water and ethanol, and dried at 80 °C.

2.4 DSSC preparation and assembling

Before coating of the photoactive material, the FTO glass substrate was cleaned in ultra-sonic bath using detergent, water and ethanol. The commercial TiO_2 paste (Dyesol) was coated using screen printing, and dried/sintered at 500 °C for 30 min. After that, the TiO_2 -coated FTO substrate was immersed in dye solution, and kept at 40 °C in the automatic shaker for 12 h. The dye-adsorbed photoelectrode was further washed with absolute ethanol, and dried in air. The prepared photo electrode was assembled with counter electrode, using Surlyn thermal adhesive film (thickness = 25 μm) as spacer. After that, the drops of the electrolyte were inserted via vacuum backfilling through the drilled hole. After filling the electrolyte, the back hole was sealed with cover glass and adhesive Surlyn.

3 Results and discussion

3.1 Reaction and growth mechanism

Although the 3D flower-like morphology of the metal sulfide has been reported by various authors, the exact mechanism

is complicated, and still not clearly understood. However, different hydrothermal temperature and precursor would lead to different crystal structure, morphology, size, unique morphology and different phase of synthesized material [21]. Usually a three-step formation mechanism possible for the cobalt and sulfur source has been proposed by researchers, which is described as follows [21, 22]: firstly in the hydrothermal procedure, cobalt and thiourea form a complex, and produce a large amount of CoS primary particles. Secondly, these primary particles are aggregated, and form solid microspheres; and finally, in the third step, larger diverse structures are obtained. It was determined that upon heating, ligand complex would finally decompose to give free Co^{2+} ions and active S^{2-} ions in the solution. Our literature review concluded that various methods and expensive precursors were used for the synthesis of metal sulfide. However, in our case, we simply used a one-step solvothermal method to grow three-dimensional CoS flower-like architecture on FTO glass. Firstly, we used cobalt nitrate and thiourea as precursor to synthesized binder-free flower-like electrode on FTO to prevent lower conductivity, which is also beneficial for the uniformity of film, which is of main concern in the DSSC device. Figure 1 b shows CoS@FTO film that is not uniformly grown, and easily leached out during simple washing.

After that, we modify our reaction system, and use aniline monomer as an adhesive in the synthesis of CoS@FTO; and to confirm the role of aniline, we check the durability of the

electrode over the FTO surface using tape test, because in practical application, stability of the electrode is the main concern. Figure 1 a clearly shows that after the addition of a negligible amount of aniline monomer, the film is stable, and this also helps to increase the conductivity of CoS@FTO, which leads to fast charge transport, and lower series of resistance of the device leads. SEM analysis shows that without the addition of aniline monomer, the 3D flower-like morphology of CoS on FTO is unstable, and easily detached from the FTO glass.

Here, we attempt to explain the synthesis mechanism of CoS@FTO with the help of the SEM images at different time duration, which explanation is well supported by previously published work [20–23]. The reactions that occur inside the hydrothermal reactor are as follows: initially, the Co^{2+} could make the precursor complex with aniline (Fig. 1 a). After that, H_2S is gradually released, due to the decomposition of thiourea, after increasing the temperature from room temperature (RT) to 200 °C. The H_2S and Co-aniline precursor complex react, and form tiny CoS nuclei. With the reaction proceeding, these tiny nuclei grow larger, so that particles with different sizes appear in the solution (Fig. 2), which is also confirmed by the SEM images of CoS after 1 h after hydrothermal synthesis. Driven by the minimization of surface free energies, the larger particles grow at the cost of the smaller ones, based on a typical Ostwald ripening process. In the subsequent process, the primary particles diffuse, and aggregate together to form solid microspheres,

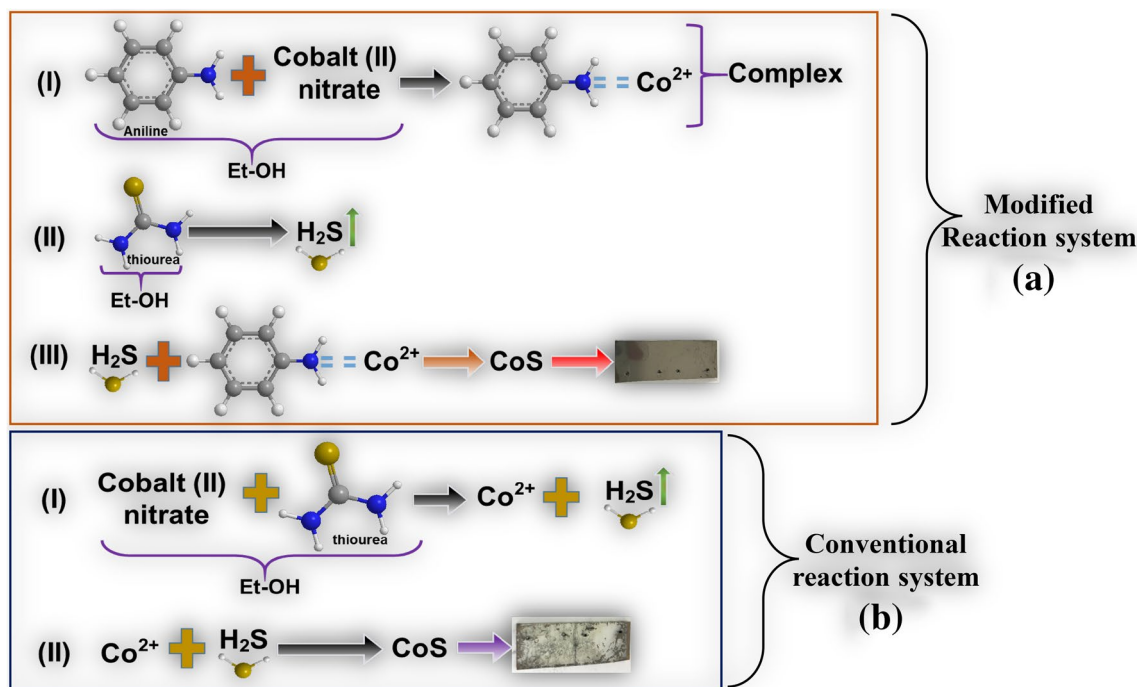


Fig. 1 The possible interaction of the initial precursor constituents **a** with aniline, and **b** without aniline

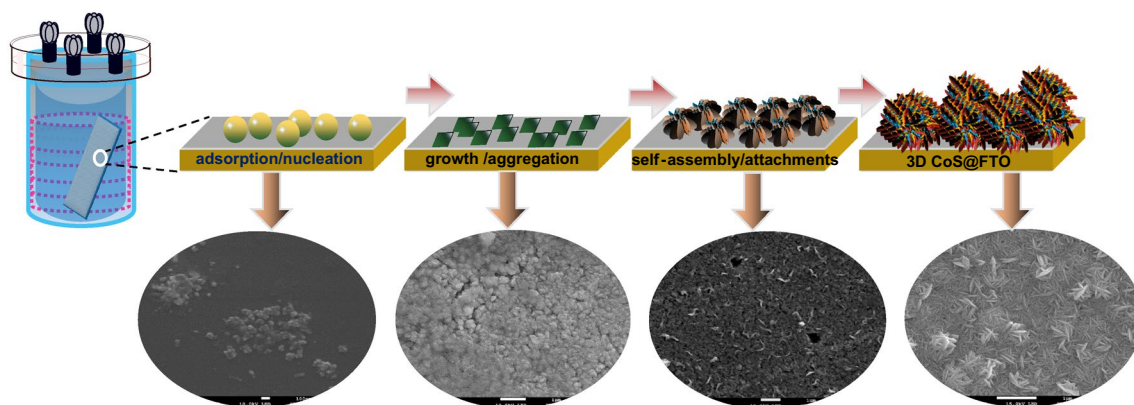


Fig. 2 Schematic of the formation mechanism of CoS@FTO. The insets show the corresponding SEM images at different steps

and the microspheres tend to cluster in groups. The surface of the microspheres acts as nucleation sites for the formation of angular CoS nanostructure, which provides many high-energy sites for nano crystalline growth. Thus, the Co-aniline complex and H_2S in the solution prefer transferring onto the surface of the sphere-like micro particles, and spontaneously nucleate on the small nanostructures. Moreover, due to the high intrinsic anisotropic properties, these initial CoS nuclei prefer to grow into nanopetals based on the precipitation solubility equilibrium in the solution. This dissolution–recrystallization process (Ostwald ripening) is a common phenomenon in the crystal growth process. When the reaction time is prolonged, the microspheres are exhausted because of mass diffusion and Ostwald ripening, and plenty of nanopetals are formed. As the Ostwald ripening process continues, the petals become thinner. Finally, a hierarchical three-dimensional flower-like morphology is formed (Fig. 2).

3.2 SEM, XRD, and XPS analysis

To understand the flower-like morphology formation process of the precursor, SEM micrography was applied to investigate the sample collected at different reaction time intervals, as shown in Fig. 2. Initially after 1 h of solvothermal treatment, some colloidal nano particles could be observed in Fig. 2, which indicates that flower-like morphology formation started from nano particle formation at the initial stage. When the reaction had proceeded for 2 h, these nano particles become dense, and of irregular size. Increasing the reaction time duration to 5 h resulted in the formation of microspheres with a combination of particles and plate-like structures, due to the aggregation of the formed particles. Figure 2 shows that after 7 h, several non-uniform plate-like structure formations for the intermediate collected sample have formed. When the reaction time was prolonged to 10 h, a huge amount of nanoplates appear, which were

interlinked together to form flower-like structure. Increasing the solvothermal time to 12 h resulted in the formation of a distinct and homogeneous three-dimensional CoS flower-like architecture assembled by uniform nanosheets that were generated on FTO glass. On the basis of the experimental SEM results and investigation of the growth mechanism, that growth mechanism is tentatively proposed and depicted. The morphology of the CoS@FTO was observed by SEM, and Fig. 3 a–c present the results to determine the structural characteristics and morphology of the as-obtained material. The SEM images at low magnification clearly show the three-dimensional flower-like morphology of the CoS@FTO, whereas the high-magnification images show that the surface of the 3D framework was uniformly covered by sheets, and these petals were connected or interlinked with each other, which significantly enhanced the surface area of the material. In addition, the TEM image presented in Figure S1 further confirmed three-dimensional flower-like morphology of the CoS@FTO.

The phase structure of the CoS@FTO was examined by XRD analysis, and further compared with the bare FTO. Figure 3 d shows that the diffraction pattern of the CoS@FTO clearly shows the presence of the characteristic peak of CoS in the present material, which can be readily indexed to the diffraction planes of (100), (101), (102), and (110). These observed diffraction planes of CoS@FTO are in close agreement with the standard diffraction of the hexagonal phase of CoS, which is the most stable form of CoS (JCPDS no. 65-8977) [1].

The chemical composition and oxidation state of the as-synthesized 3D flower-like CoS were investigated by XPS analysis. Figure 3 e shows that the Co spectrum is split into two peaks: a main peak at 778 eV, with a shoulder peak at 780 eV, indicating the oxidation state of Co^{2+} . The high-resolution S 2p XPS spectrum of CoS (Fig. 3 f) reveals the binding peaks at (161, 164.9, and 168.9) eV ($(-C-S-C-)$, $(-C=S-)$, and $(C-SO_n-C)$, respectively), which could be

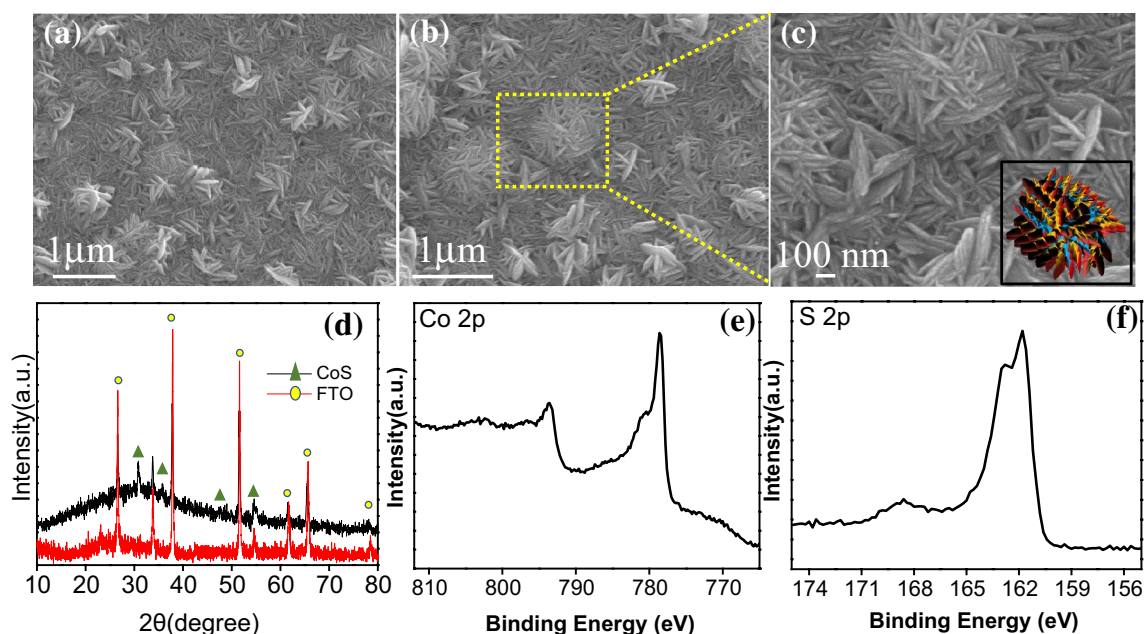


Fig. 3 a–c SEM images at different magnification (fig. c inset showing the 3D model of the CoS@FTO), d XRD pattern, e Co 2p high-resolution XPS spectrum, and f S 2p high-resolution XPS spectrum of the CoS@FTO electrode

assigned to the spin–orbit couple of S 2p_{3/2} and S 2p_{1/2}, respectively.

3.3 Electrochemical performance

The electrocatalytic reduction of the I₃[−] into I[−] over the CoS@FTO surface was examined by the cyclic voltammetry technique. The CV curve of the Pt@FTO electrode shows two distinct oxidation and reduction peaks, in which the negative pair corresponds to the redox reduction of the I[−]/I₃[−], whereas the positive pair corresponds to the I₂/I₃[−] (Fig. 4 a). Since the more common reaction in the DSSC is the reduction of the I^{3−} to I[−] over the counter electrode, we focused on the negative peak, and found that the catalytic reduction over the CoS@FTO is almost similar to that of the Pt@FTO electrode. Apart from the negative and positive pair, the peak-to-peak separation also gives insight into the catalytic activity over the electrode surface, and the electrochemical rate constant is inversely proportional to the peak-to-peak separation (E_{pp}). The E_{pp} of 0.409 was observed for the CoS@FTO, whereas the E_{pp} for the Pt@FTO was 0.417 V. The as-prepared CoS@FTO reveals similar behavior i.e. it shows two similar pairs of redox peaks in similar shape to the CV curve of the Pt@FTO electrode. However, the CoS@FTO exhibited higher current, as compared to the Pt@FTO electrode. The overall catalytic activity of the CoS@FTO might be due to the high density of the three-dimensional flower-like CoS@FTO, which provides various catalytic sites, and surface area charge transfer channels for

the electron and electrolytes to accelerate the reduction of the iodine-based electrolytes.

Figure 4 b shows the detailed results that were observed of the photovoltaic performance of the CoS@FTO and Pt@FTO in the DSSC. The photocurrent–photovoltage curve shows that the CoS@FTO exhibits similar and comparative performance to the well-known Pt@FTO electrode. The Pt@FTO exhibits the 0.746 V open-circuit voltage (V_{oc}), 12.23 mA/cm² short-circuit current density (J_{sc}), 56% fill factor (FF), and 5.97% conversion efficiency; whereas, CoS@FTO displays 0.753 V V_{oc}, 11.86 mA/cm² J_{sc}, 63.17% FF, and 5.64% conversion efficiency. The Nyquist plot was further employed to understand the charge transfer properties over the surface of the electrode and results are presented in Figure S2. The diameter of the semicircle of the CoS is smaller as compared to the Pt which indicating that the CoS has the better charge transfer rate and lower interfacial resistance over the CoS electrode surface (Figure S2). The above results clearly show that the CoS@FTO exhibits similar and comparative performance to the Pt@FTO, which may be due to the high surface area originating from the 3D flower-like morphology, and the excellent electrocatalytic activity for the reduction of electrolytes. In addition, the present obtained results were further compared with the other previously reported CoS and other typical transition metal sulfide based electrodes and their corresponding DSSC performances. Figure 4c shows that compared to the previously reported work, the present performance is higher [3, 9, 10, 18–20, 24–30].

Fig. 4 **a** CV voltammograms of CoS@FTO and Pt@FTO counter electrodes in iodine based electrolyte, **b** Current density–voltage curves of DSSCs with CoS@FTO and Pt@FTO electrode, and **c** the performance graph of the CoS@FTO in comparison with the previous results

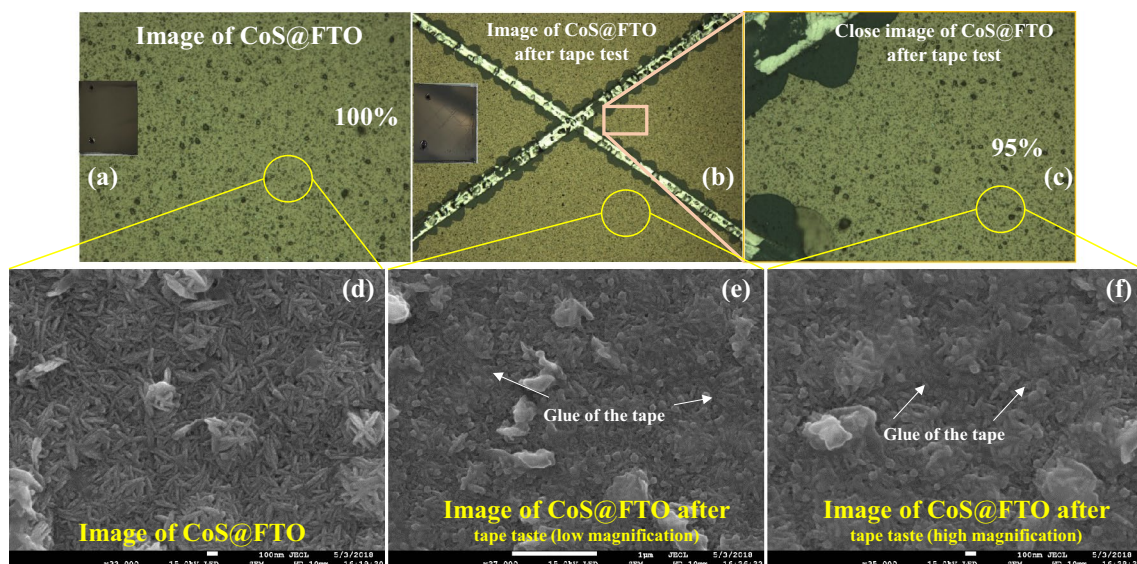
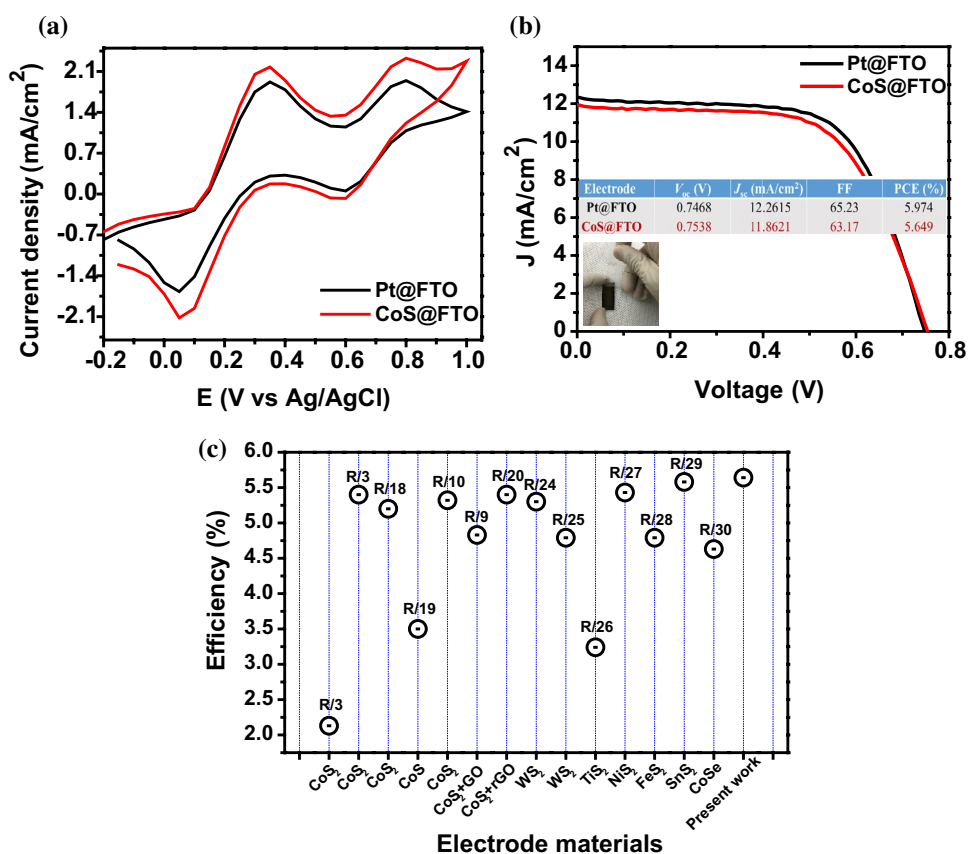


Fig. 5 Adhesion stability test images observed by optical microscopy: **a** before tape test, **b**, **c** after tape test; adhesion stability test images observed by SEM: **d** before tape test, **e**, **f** after tape test

3.4 Mechanical stability of the CoS grown at FTO

In addition to the counter electrode performance of CoS@FTO in DSSC, the stability of the electrode over the FTO

surface is also an issue of concern for practical application. In order to determine the stability of the CoS@FTO, the most widely used tape test or cross cut test was done. The as-prepared CoS@FTO electrode was first prepared by sharp

razor, in order to provide edges over the electrode surface (Fig. 5b, c and e, f). After cutting the X-like edge pattern, the whole area of the CoS coated surface was covered by strong adhesive tape, and tightly pressed. Then the tape was pulled off, and the tested area examined with the help of the microscope, and the adhesion strength was rated according to the removed amount of the coating. The examined results show that after the strong adhesive tape test, the CoS@FTO retained almost 95% of the coating (Fig. 5 c–f).

4 Conclusion

This work establishes a one-step solvothermal growth of CoS@FTO. The addition of aniline monomer provides good film deposition during the solvothermal treatment. The three-dimensional flower-like structure of the CoS as the counter electrodes provides larger surface area and interfacial contact between the electrolyte and electrode, which is advantageous for the reduction of the electrolytes over the CoS surface. The DSSC assembled using CoS as counter electrodes delivered the power efficiency of 5.64%, which is very close to the bench mark Pt catalysts (5.9%). This comparable performance of the CoS@FTO with Pt@FTO may be due to the unique 3D structure of CoS with interconnected structure, large accessible surface area, and electrocatalytic behavior of CoS. This simple and low-cost one-step synthesis method for the synthesis of metal sulfide may have enormous potential to replace the Pt counter electrode in future DSSC application.

Acknowledgements This research was supported by the Basic Science Research Program through the National Research Foundation of Korea (NRF), funded by the Ministry of Education (NRF-2015M1A2A2054996, NRF-2016R1A2B2012061). It was also supported by the Technology Development Program to Solve Climate Changes of the National Research Foundation (NRF), funded by the Ministry of Science, ICT & Future Planning (NRF-2016M1A2A2940912). This work was supported by the Dongguk University Research Fund of 2018 (S-2018-G0001-00035, S-2018-G0001-00063).

References

- J. Huo, J. Wu, M. Zheng, Y. Tu, Z. Lan, *Electrochim. Acta* **180**, 574 (2015)
- C.-W. Kung, H.-W. Chen, C.-Y. Lin, K.-C. Huang, R. Vittal, K.-C. Ho, *ACS Nano* **6**, 7016 (2012)
- J.-C. Tsai, M.-H. Hon, I.-C. Leu, *Chemistry* **10**, 1932 (2015)
- X. Wang, B. Batter, Y. Xie, K. Pan, Y. Liao, C. Lv, M. Li, S. Sui, H. Fu, *J. Mater. Chem. A* **3**, 15905 (2015)
- Y. Liao, K. Pan, Q. Pan, G. Wang, W. Zhou, H. Fu, *Nanoscale* **7**, 1623 (2015)
- X. Miao, K. Pan, G. Wang, Y. Liao, L. Wang, W. Zhou, B. Jiang, Q. Pan, G. Tian, *Chemistry* **20**, 474 (2014)
- J. Kwon, J.H. Park, *J. Electrochem. Sci. Technol.* **4**, 89 (2013)
- M.M. Rahman, H.-S. Son, S.-S. Lim, K.-H. Chung, J.-J. Lee, *J. Electrochem. Sci. Technol.* **2**, 110 (2011)
- X. Duan, Z. Gao, J. Chang, D. Wu, P. Ma, J. He, F. Xu, S. Gao, K. Jiang, *Electrochim. Acta* **114**, 173 (2013)
- S. Srinivasa Rao, C.V.V.M. Gopi, S.-K. Kim, M.-K. Son, M.-S. Jeong, A.D. Savariraj, K. Prabakar, H.-J. Kim, *Electrochim. Acta* **133**, 174 (2014)
- H. Cao, Y. Xie, Q. Feng, H. Wang, X. Wang, Z. Xu, F. Xiao, W. Zhou, K. Pan, *Int. J. Hydrogen Energy* **43**, 18832 (2018)
- X. Wang, Y. Xie, K. Pan, J. Wu, Y. Xiao, P. Yu, W. Zhou, H. Fu, *ACS Appl. Nano Mater.* **1**, 4900 (2018)
- X. Wang, Y. Xie, Z. Cai, N. Xiong, Z. Xu, M. Li, Q. Feng, W. Zhou, K. Pan, *J. Alloys Compd.* **739**, 568 (2018)
- X. Wang, Y. Xie, B. Bateer, K. Pan, Y. Jiao, N. Xiong, S. Wang, H. Fu, *ACS Appl. Mater. Interfaces* **9**, 37662 (2017)
- X. Wang, Y. Xie, B. Bateer, K. Pan, Y. Zhou, Y. Zhang, G. Wang, W. Zhou, H. Fu, *Nano Res.* **9**, 2862 (2016)
- H. Geng, L. Zhu, W. Li, H. Liu, L. Quan, F. Xi, X. Su, *J. Power Sources* **281**, 204 (2015)
- H.-J. Kim, C.-W. Kim, D. Punnoose, C.V.V.M. Gopi, S.-K. Kim, K. Prabakar, S.S. Rao, *Appl. Surf. Sci.* **328**, 78 (2015)
- J.-C. Tsai, M.-H. Hon, I.-C. Leu, *RSC Adv.* **5**, 4328 (2015)
- M. Congiu, L.G.S. Albano, F. Decker, C.F.O. Graeff, *Electrochim. Acta* **151**, 517 (2015)
- L. Sun, Y. Bai, N. Zhang, K. Sun, *Chem. Commun.* **51**, 1846 (2015)
- T. Huang, M. He, Y. Zhou, S. Li, B. Ding, W. Pan, S. Huang, Y. Tong, *RSC Adv.* **6**, 100392 (2016)
- X.-S. Hu, Y. Shen, L.-H. Xu, L.-M. Wang, Y.-J. Xing, *J. Alloys Compd.* **674**, 289 (2016)
- Q. Wang, L. Jiao, H. Du, W. Peng, Y. Han, D. Song, Y. Si, Y. Wang, H. Yuan, *J. Mater. Chem.* **21**, 327 (2011)
- C. Song, S. Wang, W. Dong, X. Fang, J. Shao, J. Zhu, X. Pan, *Sol. Energy* **133**, 429 (2016)
- B. Yang, X. Zuo, P. Chen, L. Zhou, X. Yang, H. Zhang, G. Li, M. Wu, Y. Ma, S. Jin, X. Chen, *ACS Appl. Mater. Interfaces* **7**, 137 (2015)
- Y. Duan, Q. Tang, J. Liu, B. He, L. Yu, *Angew. Chem. Int. Ed.* **53**, 14569 (2014)
- Y. Wang, S. Li, Y. Bai, Z. Chen, Q. Jiang, T. Li, W. Zhang, *Electrochim. Acta* **114**, 30 (2013)
- G. Yue, J. Wu, J.-Y. Lin, Y. Xiao, S.-Y. Tai, J. Lin, M. Huang, Z. Lan, *Carbon N. Y.* **55**, 1 (2013)
- C.-T. Li, C.-P. Lee, Y.-Y. Li, M.-H. Yeh, K.-C. Ho, *J. Mater. Chem. A* **1**, 14888 (2013)
- J. Zheng, W. Zhou, Y. Ma, W. Cao, C. Wang, L. Guo, *Chem. Commun.* **51**, 12863 (2015)

Publisher's Note Springer Nature remains neutral with regard to jurisdictional claims in published maps and institutional affiliations.